Exact solvability of the Gross-Pitaevskii equation for general potentials with bound states

M. Mirón and E. Sadurní

Instituto de Física, Benemérita Universidad Autónoma de Puebla, Apartado Postal J-48, 72570 Puebla, México.

Received 28 January 2025; accepted 7 January 2026

In this paper we present the analytic solution of the bound state problem for the Gross-Pitaevskii (GP) equation in 1D and its properties, in the presence of external potentials such as finite square wells and attractive Dirac deltas, as well as stable solitons for repulsive defects. We show that the GP equation can be mapped to a first-order non-autonomous dynamical system, whose solutions can sometimes be written in terms of known functions. The formal solutions of this non-conservative system can be written with the help of Glauber-Trotter formulas or a series of ordered exponentials in the coordinate x. With this we illustrate how to solve any nonlinear problem based on a construction due to Mello and Kumar for the linear case (layered potentials). For the benefit of the reader, we comment on the difference between the integrability of a quantum system and the solvability of the wave equation.

Keywords: Bound states; Gross-Pitaevskii equation; solitons; integrability.

DOI: https://doi.org/10.31349/RevMexFis.72.040401

1. Introduction

In this paper we employ a method of quadratures to solve the nonlinear Schrödinger equation in 1D for bound states in a general potential, *i.e*. solitons with discrete spectra. It is sometimes suggested that only a finite list of potentials allows analytical expressions for stationary waves and energies. This statement is usually motivated by the factorization method in the sense of Infeld and Hull [1]. Here, however, we give a formal solution to any stationary problem with bound states by working out the specific cases of constant piecewise potentials and point-like defects; then the results are generalized to any potential by taking the limit of an infinite number of coalescent regions. This shows that explicit wave functions can always be found, as well as transcendental equations that determine the energy eigenvalues, albeit the need of numerical evaluations for obtaining the spectrum. This method is in compliance with the definition of boundary conditions at infinity.

From the first treatments of the nonlinear Schrödinger equation [2–9] it was already evident that nonlinearities could pose additional challenges for the computation of waves and spectra. The impact of new analytical solutions of this problem reaches many areas with diverse applications [10–15]. Although it is known that the Jacobi Elliptic functions solve the nonlinear equation with piecewise constant external interactions [16,17], the method of wave function matching across boundaries is applicable only when full multi-parametric solutions are given explicitly; in this paper, we show that this can be done by our quadrature method. In the linear case, there is a counted list of potentials with closed solutions for energies and wave functions [18–22], as well as their supersymmetric extensions [23], but so far nothing has been reported for the Gross-Pitaevskii (GP) equation (we note that in the Thomas-Fermi limit there are explicit forms of the solution, but always in approximate form).

In order to put our contribution in context, it is important to mention that the most general form of stationary solutions for the linear case is simply given by the 2×2 scattering matrix and its pole structure, even for bound states with vanishing conditions at infinity and purely imaginary poles in the k plane. Formally, one can write the solutions of second-order differential equations by mapping the system to a two-dimensional dynamical problem [24, 25] of a lesser degree, *i.e*. a vector first-order equation. The idea of interpreting the coordinate x as a quasi-time was recently given in [16]. For the case of a general piecewise potential, gluing all pieces together by boundary matching can be done with square potentials, as well as a series of Dirac deltas, whichever is convenient. It is important to underscore that any measurable potential can be approximated arbitrarily well by this procedure, as indicated later in Eq. (30), where the results are guaranteed by Lebesgue integration. For the linear problem, the corresponding energy-dependent Green's functions and their connection with the scattering matrix are well known [26–28], but in the nonlinear case there are no such constructions; the Green's function is not available. It is interesting to note that Mello and Kummar indicated a layered construction for the general scattering problem [29] that, for convenience, can be reduced to a differential equation for the *scattering matrix* and not for the *wave function*. Now, in a similar construction, we generalize the treatment for the nonlinear case and the wave function.

Perhaps the most important motivation of these studies, in recent times, belongs to the quantum mechanical realization of the GP equation in Bose-Einstein condensation (BEC) and the existence of multiple nonlinear bound states in a potential well or lattice trap [30]. These bound solitons, men-

tioned in [16, 31, 32], undergo multilevel transitions that may be employed in the construction of qubits, qutrits and the like. Various numerical methods to attack the problem are given in [33–36], also in connection with spinorial BEC generalizations and the application of magnetic fields. The present study of the 1D GPE is well supported and motivated by experimental realizations of cigar-shaped BECs. Some of the most representative reports on the field are [37–40].

Structure of this paper: In Sec. 2 we briefly review the quadrature method. In Sec. 3 we solve the bound state problem for a delta defect and a square well potential using Jacobi Elliptic functions. The energies are obtained by solving a transcendental equation with the graphic method. In Sec. 4 we generalize the method to arbitrary potentials in the continuous limit of layered defects; we do this for the linear as well as the nonlinear problem, arriving at a dynamical set of equations in the spatial coordinate. In Sec. 5 we discuss the general solutions in the context of classical and quantum-mechanical integrability. In Sec. 6 we provide a detailed comparison between our method and traditional Runge-Kutta implementations for boundary value problems; in this section we also comment on the connection with BECs. Conclusions are drawn in Sec. 7.

2. Gross-Pitaevskii equation

In the description of a stationary-state BEC in a static trap given by a potential $V_{\rm ext}(x)$, we deal with the time-independent differential equation

$$\left\{-\frac{\hbar^2}{2m}\frac{d^2}{dx^2}+g|\phi(x)|^2+V_{\rm ext}(x)\right\}\phi(x)=E\phi(x). \quad (1)$$

This is deduced from a mean field theory considering only contact interactions, the particles are in the same state, and the state function of a single particle is sufficient to describe the complete bosonic system. Here, m is the particle's mass, $\hbar$ is the reduced Planck constant, $E^{\text{parameter}}$ is the spectral parameter that generalizes the energy of the stationary state, and g is related to the scattering length a of $s-$state through $g_{3\rm D}=(4\pi\hbar^2 a)/m$ [2] and its dimensional reduction in the weakly-interacting limit is $g=g_{1\rm D}=g_{3\rm D}/2\pi a_\perp^2$ in terms of the transverse width $a_\perp$ of an elongated trap [41, 42][ii]. The map to a dynamical system with quasi-time $\tau=\sqrt{2m}x/\hbar$ (proportional to x) is defined by a complex coordinate $X(\tau)=\phi(x)$ and its velocity $\dot X(\tau)=d\phi(x)/d\tau$. A first-order differential equation emerges, involving a complex vector with components $(\dot X, X)$:

$$\frac{d}{d\tau}\begin{pmatrix}\dot X\\ X\end{pmatrix}=\begin{pmatrix}0 & V-E+g|X|^2\\ 1 & 0\end{pmatrix}\begin{pmatrix}\dot X\\ X\end{pmatrix}. \quad (2)$$

It is important to note that the complex character of $X(\tau)$ makes the system two-dimensional, and in this kind of mapping, the polar coordinates (r,φ) in the complex plane represent the density $r^2=|\phi|^2$ and the phase $\varphi=\arg(\phi)$, *i.e.*, $X=\phi=re^{i\varphi}$. If we substitute in Eq. (2), we obtain

$$\ddot r-r\dot\varphi^2-(V-E-gr^2)r=0,\ 2\dot r\dot\varphi+r\ddot\varphi=0. \quad (3)$$

When the potential V is constant in a region, these equations are autonomous and possess two conserved quantities, U and J, which correspond to energy and angular momentum in our mechanical analogy. The use of such integrals of the motion lowers the degree of differential equations as follows [16]

$$U=\frac{1}{2}\dot r^2+\frac{1}{2}r^2\dot\varphi^2+\frac{1}{2}(E-V)r^2-\frac{1}{4}gr^4,\ r^2\dot\varphi=J. \quad (4)$$

In fact, computing $\dot U$ and $\dot J$ leads directly to (3). In our compact notation with X, the constant U henceforth known as quasi-energy functional, is conserved (in τ or x) along the solutions $X(\tau)$:

$$U=|\dot X|^2/2+\Phi[X], \quad (5)$$

with $\Phi[X]=(E-V)|X|^2/2-g|X|^4/4$.

In general, φ does not vanish, and its variation can be identified with the conserved probability current $J=r^2d\varphi/dx,\ dJ/dx=0$, which is in full parallel with the conserved angular momentum of a particle in a planar space under the influence of an isotropic potential $\Phi[r]=(E-V)r^2/2-gr^4/4$. Using the separability of the problem, the radial coordinate *feels* the action of an effective potential with a centrifugal barrier $\Phi_{\rm eff}[r]=\Phi[r]+J^2/2r^2$. As we have shown in previous work [16], scattering solutions necessitate a non-vanishing φ and its inherent phase shift, but since bound states are the main focus of the present discussion, we can impose $\varphi=0$.

It is important to remember that a key condition for the existence of bound solutions is a vanishing current in 1D. This comes from the continuity equation applied to nonlinear problems, including solitons of the GPE. Free solitons [43], on the other hand, are constituted by a localized envelope $u(x-vt)$ and the phase factor of a traveling wave $\exp[i(mvx-mv^2t/2)/\hbar]$, but since our interest is to find bound solitons, *i.e.*, trapped by a static potential, both the traveling part and the complex phase factor are eliminated in this paper by setting $v=0$, leaving us with real wave functions.

The quadrature method consists in evaluating the integral for the period or lapse τ and solve for r alone, where E and r_0 are the only parameters:

$$\tau=\int_{r_0}\frac{dr}{\sqrt{2(U-\Phi_{\rm eff}[r])}}. \quad (6)$$

This greatly simplifies the equations above, as well as the effective potential; we have $\Phi_{\rm eff}[r]=\Phi[r]$ and X real. Under a change of variables $\eta=r^2$, this quadrature (6) is transformed into the integral representation of the Jacobi Elliptic function [16], where the limits of integration are compatible with the turning points of the potential Φ, *i.e.*, where the expression inside the radical is a third-order polynomial $P(\eta)$

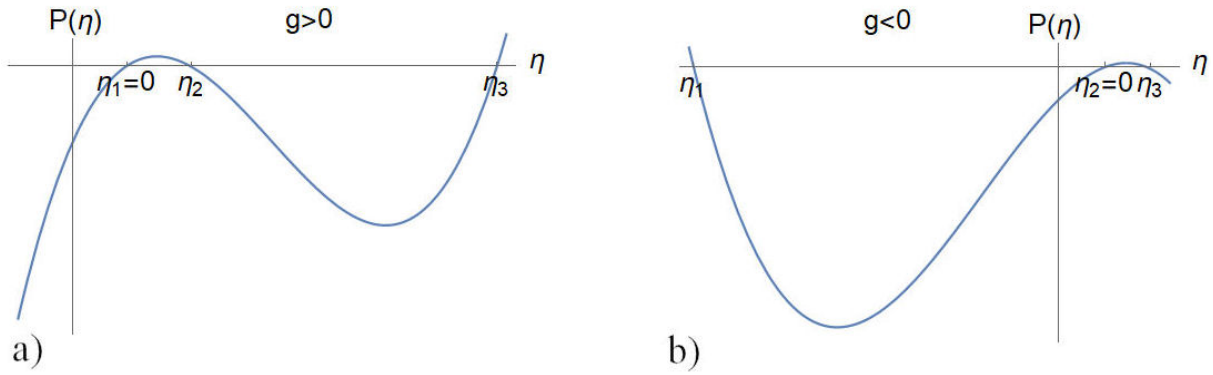

FIGURE 1. Roots of the polynomials that define the elliptic Jacobi functions.

with real roots and positive values. Depending on the sign of g, the polynomial $P(\eta)$ has a specific ordering of its roots $\eta_i, i = 1, 2, 3$. This is shown in Fig. 1. In what follows, we illustrate the method of solution for particles bound by simple potentials using boundary matching conditions.

3. Nonlinear bound states in delta and box potentials

Two simple models are solved in order to illustrate the boundary matching method in nonlinear systems; from these two examples, we may construct more complicated cases.

3.1. Dirac delta

We solve the GP equation for bound states in 1D. As a result, we shall find that, contrary to the linear case, positive Dirac deltas can support bound states up to a threshold negative coupling g. Similarly, a negative delta may lose its binding capabilities if a positive nonlinear coupling g is sufficiently strong. We start with the equation

$$\left\{-\frac{d^2}{d\tau^2} + V_{\text{ext}}(\tau) + \gamma\psi^2(\tau)\right\}\psi(\tau) = E\psi(\tau), \quad (7)$$

where a convenient rescaling is used $\tau = \sqrt{2m}x/\hbar$, $\bar{\alpha} = \sqrt{2m}\alpha/\hbar$, $\gamma = \sqrt{2m}g/\hbar$, $V_{\text{ext}}(\tau) = \bar{\alpha}\delta(\tau)$, $\psi = (2m)^{1/4}\phi/\sqrt{\hbar}$. We divide the problem into two regions: 1 denotes $\tau < 0$ and 2 corresponds to $\tau > 0$. Then the matching conditions are given by $\psi_2(0) = \psi_1(0)$, $\dot{\psi}_2(0) = \dot{\psi}_1(0) + \bar{\alpha}\psi_1(0)$. The following two cases can be distinguished: generalized bright solitons and logarithmic quadratures, which are shown below.

3.1.1. *Bright solitons*

For bright solitons, $E < 0$ and $\gamma < 0$, there are bound states given by

1. *Repulsive defect*

$$\psi_{\bar{\alpha}>0}(\tau) = \begin{cases} \sqrt{\frac{2E}{\gamma}}\,\text{sech}\left(\sqrt{|E|}(\tau+\bar{\tau})\right) & \text{if} \quad \tau < 0 \\ \sqrt{\frac{2E}{\gamma}}\,\text{sech}\left(\sqrt{|E|}(\tau-\bar{\tau})\right) & \text{if} \quad \tau > 0 \end{cases} \quad (8)$$

with $\bar{\alpha} = 2\sqrt{|E|}\tanh\left(\sqrt{|E|}\bar{\tau}\right)$ and $0 \leq \bar{\alpha} \leq 2\sqrt{|E|}$.

2. *Attractive defect*

$$\psi_{\bar{\alpha}<0}(\tau) = \begin{cases} \sqrt{\frac{2E}{\gamma}}\,\text{sech}\left(\sqrt{|E|}(\tau-\bar{\tau})\right) & \text{if} \quad \tau < 0 \\ \sqrt{\frac{2E}{\gamma}}\,\text{sech}\left(\sqrt{|E|}(\tau+\bar{\tau})\right) & \text{if} \quad \tau > 0 \end{cases} \quad (9)$$

with $\bar{\alpha} = -2\sqrt{|E|}\tanh\left(\sqrt{|E|}\bar{\tau}\right)$ and $-\infty \leq \bar{\alpha} < 0$.

In both cases

$$E = -\frac{\bar{\alpha}^2}{4} + \frac{\gamma}{2}\psi^2(0). \quad (10)$$

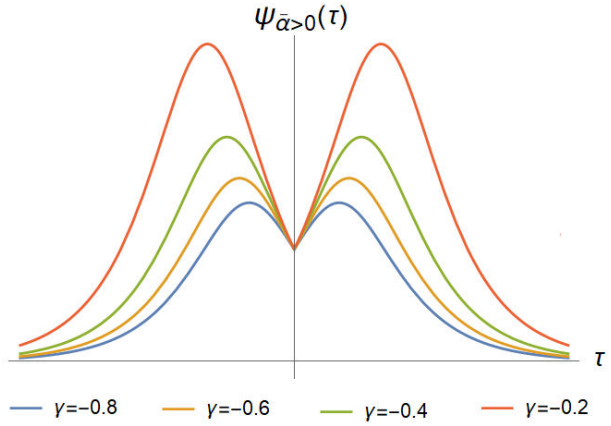

FIGURE 2. Bright solitons in repulsive barrier. $\psi_{\alpha>0}(0)$ and α are fixed. When $\gamma \to 0$, $\psi_{\bar{\alpha}>0}(-\bar{\tau}) = \psi_{\bar{\alpha}>0}(\bar{\tau}) \to \infty$ and $\bar{\tau} \to \infty$.

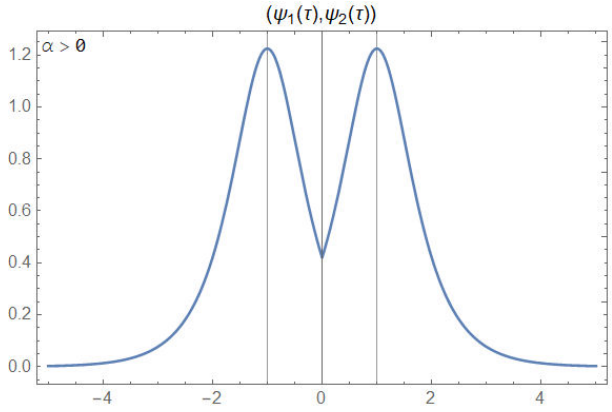

FIGURE 3. Bright solitons. Repulsive defect and negative coupling. The bound state is repelled but not destroyed by the point-like potential.

The results are displayed in Figs. 2 and 3, where the effect of the delta potential changes the shape of the soliton according to its sign. In the repulsive case, we observe that in the limit when $\gamma \to 0$, the energy remains negative $E \to -\alpha^2/4$, if the amplitude at the defect is kept constant, for which $\psi_{\bar{\alpha}>0}(-\bar{\tau}) = \psi_{\bar{\alpha}>0}(\bar{\tau}) \to \infty$ and $\bar{\tau} \to \infty$, *i.e.*, the amplitude and the two maxima of the soliton increase, as we can see in Fig. 2.

3.1.2. *Solution associated to a logarithmic quadrature*

Here we have $\bar{\alpha} < 0$, $E < 0$ and $\gamma > 0$, representing bound states. In this case, the equation for quasi-energy conservation becomes

$$U_1 = \frac{1}{2}\dot{\psi_1}^2(\tau) + \Phi_{\text{eff}}(\psi_1),\ \tau < 0; \tag{11}$$

$$U_2 = \frac{1}{2}\dot{\psi_2}^2(\tau) + \Phi_{\text{eff}}(\psi_2),\ \tau > 0; \tag{12}$$

$$\Phi_{\text{eff}}(\psi_i) = \frac{1}{2}E\psi_i^2(\tau) - \frac{\gamma}{4}\psi_i^4(\tau). \tag{13}$$

The only admissible solution is obtained with $U_1 = 0 = U_2$, $\psi_1(0) = \psi_2(0) = \psi_0$, $\dot{\psi}_1(0) = (\bar{\alpha}\psi_0)/2 = -\dot{\psi}_2(0)$, $\psi_0 = \sqrt{(\bar{\alpha}^2 - 4|E|)/2\gamma}$, *i.e.*,

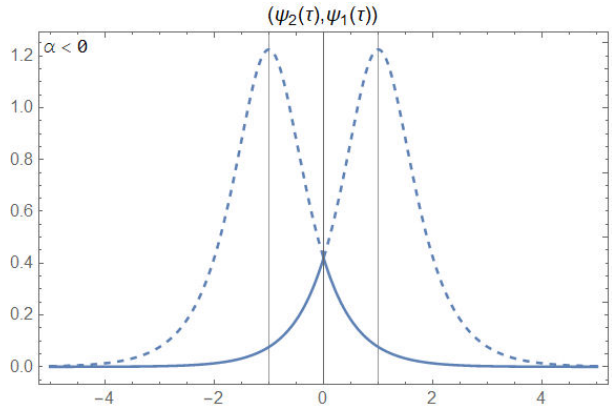

FIGURE 4. Bright solitons. Attractive defect and negative coupling. Both contributions make the binding mechanism stronger.

$$-\sqrt{|E|}|\tau| = \log\left\{\frac{(1+2\sqrt{|E|})\psi(\tau)}{\sqrt{1-4|E|}\left(\sqrt{\frac{2|E|}{\gamma}} + \sqrt{\psi^2(\tau) + \frac{2|E|}{\gamma}}\right)}\right\}, \tag{14}$$

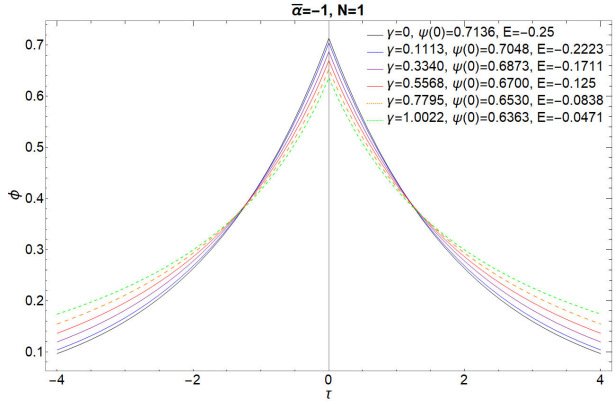

FIGURE 5. Wave functions computed with a logarithmic quadrature, valid for positive nonlinear coupling. When the densities are properly normalized, the localization length of $\gamma = 0$ and $\gamma > 0$ can be compared, and the loosely bound state can be identified by its larger width.

under the conditions $\bar{\alpha} \leq -\sqrt{2\gamma}\psi_0 = \alpha_{\text{crit}}$, $E = \gamma\psi_0^2/2 - \bar{\alpha}^2/4 \leq 0$. From (14) it is possible to recover the explicit wave function in terms of exponentials or hyperbolic functions, by trivially solving for $\psi(\tau)$. We show the results in Fig. 5. The intensity parameter γ of the nonlinearity modifies the width of the soliton, hence the localization of the wave, for a fixed $\bar{\alpha}$.

It is important to note that bound states exist if $\bar{\alpha}$ satisfies the inequalities above. This is in sheer contrast with the linear case, where any attractive potential in 1D is able to bind a particle (in 2D or higher dimensions, an attractive potential needs a critical depth to produce at least one bound state). The nonlinear case demands sufficient attraction to surpass the positive contribution $\gamma\phi_0^2$.

3.2. Square box

The boundary matching method divides the problem into three regions; 1 and 3 correspond to the exterior of the trap and 2 corresponds to the interior. As in the linear case, the continuity of the wave function and its derivative provide a transcendental equation for the allowed energy eigenvalues. For the nonlinear problem, this equation is a generalization of the familiar relation $k\tan k = \text{const}$ in the linear case, and shall be derived in terms of Jacobi amplitudes below. The graphic method of solution will be presented as well. The GP equation with a square box potential is given by

$$\left\{-\frac{d^2}{d\tau^2} + g\phi^2(\tau) + V_{\text{ext}}(\tau)\right\}\phi(\tau) = E\phi(\tau), \qquad \tau = \frac{\sqrt{2m}}{\hbar}x, \tag{15}$$

$$V_{\text{ext}}(\tau) = \begin{cases} -V_0 & \text{if} \quad |\tau| \leq \frac{\sqrt{2m}}{\hbar}x_0 = \tau_0 \\ \\ 0 & \text{if} \quad |\tau| > \frac{\sqrt{2m}}{\hbar}x_0 = \tau_0 \end{cases}, \qquad V_0 > 0. \tag{16}$$

The quasi energy in the three regions and the effective potential are

$$U_i = \frac{1}{2}\dot{\phi}_i^2(\tau) + \Phi_{\text{eff}}[\phi_i(\tau)] = \text{const.}, \tag{17}$$

$$\Phi_{\text{eff}}[\phi_i(\tau)] = -\frac{g}{4}\phi_i^4(\tau) + \frac{1}{2}[E - V(\tau)]\phi_i^2(\tau), \tag{18}$$

where $i = 1$, 2 and 3. We define $\phi_1(\tau)$ and U_1 in $\tau < -\tau_0$, $\phi_2(\tau)$ and U_2 in the region $-\tau_0 \leq \tau \leq \tau_0$, and $\phi_3(\tau)$ and U_3 in $\tau_0 < \tau$. The plots of the effective potentials are similar to the well-known *Mexican-hat* shape and are shown in Figs. 6 and 7.

The boundary matching relations are, in this case, strictly continuous: $\phi_1(-\tau_0) = \phi_2(-\tau_0)$, $\dot{\phi}_1(-\tau_0) = \dot{\phi}_2(-\tau_0)$, $\phi_2(\tau_0) = \phi_3(\tau_0)$ and $\dot{\phi}_2(\tau_0) = \dot{\phi}_3(\tau_0)$. Since the external potential is symmetric, there are two families of solutions given by symmetric functions, which fulfill $\dot{\phi}_2(0) = 0$ and antisymmetric functions, with the property $\phi_2(0) = 0$. Then the two cases $g > 0$ and $g < 0$ are treated separately as indicated in the following.

3.2.1. *Positive nonlinear coupling g*

Using the elliptic integral and consistency with matching relations at $\pm\tau_0$ leads, for $\tau \leq -\tau_0$, to

$$-\sqrt{|E|}(\tau_0 + \tau) = \log\left\{\frac{\left[\sqrt{\frac{2|E|}{g}} + \sqrt{\phi_1^2(\tau) + \frac{2|E|}{g}}\right]}{\left[\sqrt{\frac{2|E|}{g}} + \sqrt{\phi_1^2(-\tau_0) + \frac{2|E|}{g}}\right]}\frac{\phi_1(-\tau_0)}{\phi_1(\tau)}\right\}, \tag{19}$$

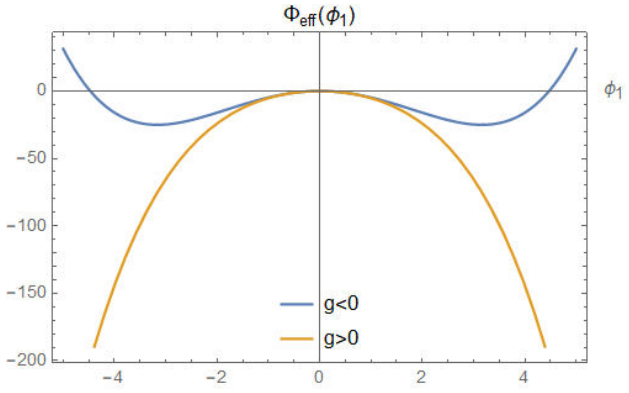

FIGURE 6. Effective potential Φ_{eff} outside of the well V_{ext}.

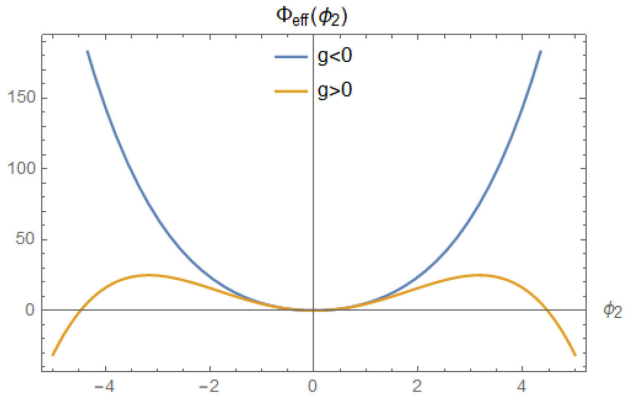

FIGURE 7. Effective potential Φ_{eff} inside of the well V_{ext}.

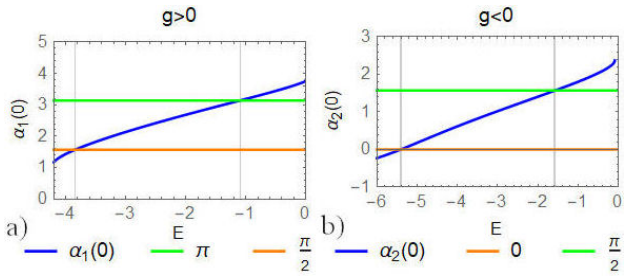

FIGURE 8. Energy curves for the graphic method. Upper panel, $g > 0$: $V_0 = 6$, $g = 1$, $\phi_0 = 0.5127$, $\tau_0 = 1$. Lower panel, $g < 0$: $V_0 = 6$, $g = -1$, $\phi_0 = 0.4310$, $\tau_0 = 1$.

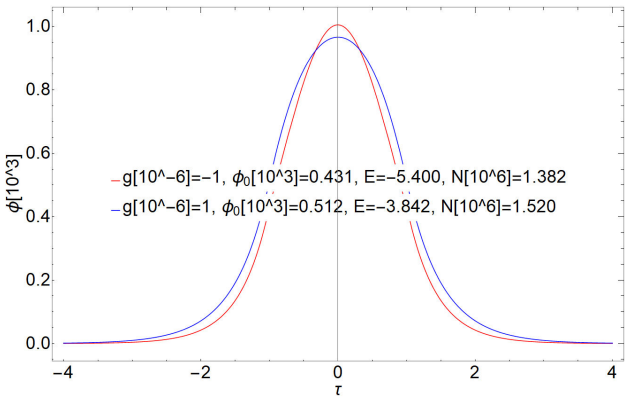

FIGURE 9. Ground state for both coupling cases. The curvatures display qualitatively different features.

while $-\tau_0 \leq \tau \leq 0$ yields

$$\phi_2(\tau) = \sqrt{\eta_2}\cos\{\alpha_1(\tau)\},$$
$$\alpha_1(\tau) = \mathrm{Am}\left[\sqrt{\frac{g\eta_3}{2}}(\tau+\tau_0) + \mathrm{F}\left(\arcsin\left\{\frac{\phi_1(-\tau_0)}{\sqrt{\eta_2}}\right\}, \sqrt{\frac{\eta_2}{\eta_3}}\right), \sqrt{\frac{\eta_2}{\eta_3}}\right] - \frac{\pi}{2}. \tag{20}$$

Here, the roots η associated with the turning points of Φ are given by

$$\eta_1 = 0, \qquad \eta_2 = \frac{E+V_0}{g} - \sqrt{\left(\frac{E+V_0}{g}\right)^2 - \frac{2V_0}{g}\phi_1^2(-\tau_0)},$$
$$\eta_3 = \frac{E+V_0}{g} + \sqrt{\left(\frac{E+V_0}{g}\right)^2 - \frac{2V_0}{g}\phi_1^2(-\tau_0)}. \tag{21}$$

For the symmetric case, we make use of the cosine function of α in the interior, giving rise to the energy quantization condition $\alpha_1(0) = n\pi$, $n = 0, 1, 2, ...$, and for the antisymmetric case $\alpha_1(0) = (n + 1/2)\pi$, $n = 0, 1, 2, ...$ These conditions are derived here for the first time, and they lead to the graphic method displayed in Figs. 8 and 9, where α is plotted against E, and its intersection with the quantized values yields the discrete energies sought for bound states.

3.2.2. Negative nonlinear coupling g

We proceed as in the previous case, but with different locations for the roots of $P(\eta)$. For $\tau \leq -\tau_0$, we have:

$$\phi_1(\tau) = \sqrt{\frac{2E}{g}}\,\mathrm{sech}\left[\sqrt{|E|}(\tau_0+\tau) + \mathrm{arcsech}\left(\sqrt{\frac{g}{2E}}\phi_1(-\tau_0)\right)\right], \tag{22}$$

and in the region $-\tau_0 \leq \tau \leq 0$,

$$\phi_2(\tau) = \sqrt{\eta_3}\cos\{\alpha_2(\tau)\},$$
$$\alpha_2(\tau) = \mathrm{Am}\left[\sqrt{\frac{|g|(\eta_3-\eta_1)}{2}}(\tau+\tau_0) - \mathrm{F}\left(\arcsin\left\{\sqrt{\frac{\eta_3-\phi_1^2(-\tau_0)}{\eta_3}}\right\}, \sqrt{\frac{\eta_3}{\eta_3-\eta_1}}\right), \sqrt{\frac{\eta_3}{\eta_3-\eta_1}}\right], \tag{23}$$

with the following explicit forms of the turning points:

$$\eta_1 = \frac{E+V_0}{g} - \sqrt{\left(\frac{E+V_0}{g}\right)^2 + \frac{2V_0}{|g|}\phi_1^2(-\tau_0)}, \qquad \eta_2 = 0,$$
$$\eta_3 = \frac{E+V_0}{g} + \sqrt{\left(\frac{E+V_0}{g}\right)^2 + \frac{2V_0}{|g|}\phi_1^2(-\tau_0)}. \tag{24}$$

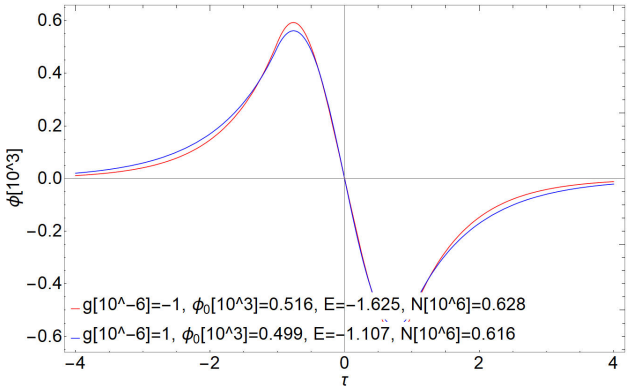

FIGURE 10. First excited state for both cases, when values of g and V allow its existence.

For the symmetric case, we now have the following quantization condition $\alpha_2(0) = n\pi$, $n = 0, 1, 2, ...$, while antisymmetric waves require the modified relation $\alpha_2(0) = (n + 1/2)\pi$, $n = 0, 1, 2, ...$ We note here that the symmetric quantum number starts at $\alpha = 0$, but this is consistent with the previous case $g > 0$ in the limit $g \to 0$, *i.e.*, the energy curves for the ground state are continuous. Note, however, that fixing the value of the wave functions at $\pm\tau_0$ forces all solutions to depend on this specific amplitude (contrary to the linear case, where overall scales of wave functions are irrelevant) and they are not immune to normalization. Although it is possible to use the total number of particles $\int dx|\phi|^2 = N$ as a parameter, this lengthy expression shall be avoided here for simplicity. As a consequence, the energy levels *are* continuous functions of g, but their slope exhibits a *kink* at $g = 0$, as can be shown explicitly by differentiating the quadrature with respect to g and employing the chain rule. We provide further comment on this below. The resulting wave functions are plotted in Figs. 8, 9 and 10 for the ground state and first excited state. The curvature changes significantly as a function of g, as well as the width of the distributions (the binding capabilities of the potential depend on the sign of g and can be characterized by a typical localization length conveniently defined by the second moment of the distribution).

In Fig. 11 we show the evolution of energy levels with the nonlinear coupling. As expected, there is always a critical value of $g > 0$ for which V cannot bind a particle, as the energy curves reach $E = 0$ at the top of the plot. We can also observe the kink in the curve E vs g at $g = 0$. The curves are continuous, but their derivative has a jump in the transition between attractive and repulsive self-interactions. This can be explained easily by means of the quadrature, since for symmetric and antisymmetric bound states, the functions $\alpha_1(0)$ and $\alpha_2(0)$ are parameterized in different ways according to the sign of g; meanwhile g is contained in both arguments of the elliptic functions $F(\ ,\ )$ and $\mathrm{Am}(\ ,\ )$ and we must keep track of such a dependence when computing the derivative with respect to g at $g = 0$. When $g \to 0$, we see that $\alpha_1(0) = \alpha_2(0)$ but $d\alpha_1(0)/dg \neq d\alpha_2(0)/dg$.

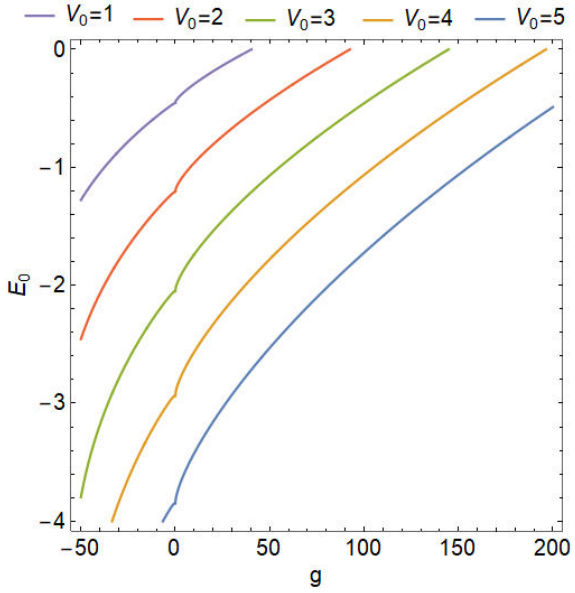

FIGURE 11. Ground state energy vs coupling for different depths.

4. Formal solution of the GP equation with general potential

Our interest is to solve the GPE for a variety of potentials that support bound states, taking advantage of the previous results. Although such cases seem to be too specialized (isolated wells or barriers), they can be employed constructively to approach any other problem. This establishes a clear connection with the general purpose of this paper. The best way to proceed is by defining a general potential in the sense of measurable functions, even for the linear case. The method generalizes the transfer matrix to a nonlinear set of recurrences between free solutions valid in interstitial regions. For the benefit of the reader, we start with the linear case and then move on to GPE via Jacobi elliptic functions. In addition, the boundary matching method is supplemented by the reduction to phase-space variables as described in (2). In this sense, the question of solvability and integrability for general potentials is better put into context, but the details are left for Sec. 5..

Indeed our phase-space differential equations (5.) are non-autonomous and their integration is given only through iterative series. The existence of solitons or localized solutions requires, in general, the existence of critical points of such dynamical systems. These are not trivial for GPE. Furthermore, the integral form of the equation is not useful *per se* before iteration. Therefore, the culmination of our treatment comes in the form of a composition law of ordered exponentials that can be fed from the analytical solutions for the case $g = 0$, giving rise to expressions of the Glauber-Trotter type [44] for products of operators. This shall be demonstrated below.

It is important to mention that our novel method is reduced to the constructive form of the scattering matrix explained by Mello *et al.* [29]; in the linear case, it is enough

to analyze the transmission and reflection coefficients in the plane of complex energies to obtain the solutions according to their boundary conditions. Here we must go one step further by generalizing the use of the scattering matrix (non-existent for GP) and finding the most general possible wave with parametric dependence on the energy.

Let the external potential be given by the continuous limit of a Dirac comb

$$V_{\rm ext}(x) = \sum_{i=0}^{N} v_i \delta(x - x_i), \tag{25}$$

with the definitions $v_i = V_i \Delta x = V_{\rm eff}(x_i)\Delta x$, $x_i = i\Delta x + x_0$, and $\Delta x = L/N$; L is the range or support of the external potential. By rescaling Eq. (1), for bound states or solitons ϕ, we obtain

$$\left\{ -\frac{d^2}{d\tau^2} + g\phi^2(\tau) + \sum_{i=0}^{N} v_i' \delta(\tau - \tau_i) \right\} \phi(\tau) = E\phi(\tau), \tag{26}$$

with $\tau = lx$, $l = \sqrt{2m}/\hbar$, $v_i' = \bar{V}_i \Delta\tau$, and since $\Delta\tau = l\,\Delta x$, the potential is not rescaled, *i.e.*, $\bar{V}_i = V_i = V_{\rm eff}(x_i)$. The continuity of the wave function and the discontinuity in its derivative give us the relations

$$\phi_{i+1}(\tau_i) = \phi_i(\tau_i), \tag{27}$$

$$\dot{\phi}_{i+1}(\tau_i) = \dot{\phi}_i(\tau_i) + v_i' \phi_i(\tau_i), \tag{28}$$

$$\phi_i = \phi_i(\tau), \qquad \tau_{i-1} \le \tau \le \tau_i, \qquad i = 1, ..., N. \tag{29}$$

In the continuous limit, we recover any desired potential V whose integral is well-defined. We have

$$\lim_{N\to\infty,\, \Delta\tau\to 0} \sum_{i=1}^{N} \Delta\tau V_i \delta(\tau - \tau_i) = \int d\tau' V(\tau')\delta(\tau - \tau') = V(\tau). \tag{30}$$

Our approach is then well justified.

4.1. Linear case

We consider first $g = 0$. In the interstitial region, between successive deltas, the solution is given by $\phi_i(\tau) = A_i \sin(\sqrt{E}\tau - \alpha_i)$, with α_i and A_i real functions. The boundary matching conditions are

$$A_{i+1} \sin(\sqrt{E}\tau_i - \alpha_{i+1}) = A_i \sin(\sqrt{E}\tau_i - \alpha_i), \tag{31}$$

$$\sqrt{E} A_{i+1} \cos(\sqrt{E}\tau_i - \alpha_{i+1}) = \sqrt{E} A_i \cos(\sqrt{E}\tau_i - \alpha_i) + V_i \Delta\tau A_i \sin(\sqrt{E}\tau_i - \alpha_i). \tag{32}$$

In the continuous limit we have $A_i \to A(\tau)$, $\alpha_i \to \alpha(\tau)$, $A_{i+1} \to A(\tau + \Delta\tau)$, and $\alpha_{i+1} \to \alpha(\tau + \Delta\tau)$, such that

$$A(\tau + \Delta\tau) \sin(\sqrt{E}\tau - \alpha(\tau + \Delta\tau)) = A(\tau) \sin(\sqrt{E}\tau - \alpha(\tau)), \tag{33}$$

$$\sqrt{E} A(\tau + \Delta\tau) \cos(\sqrt{E}\tau - \alpha(\tau + \Delta\tau)) = \sqrt{E} A(\tau) \cos(\sqrt{E}\tau - \alpha(\tau)) + V(\tau)\Delta\tau A(\tau) \sin(\sqrt{E}\tau - \alpha(\tau)). \tag{34}$$

A two-component vector can accommodate the two rows above, with the definition

$$\mathbf{r}(\tau) = \begin{pmatrix} \sqrt{E} A(\tau) \cos\left(\sqrt{E}\tau - \alpha(\tau)\right) \\ A(\tau) \sin\left(\sqrt{E}\tau - \alpha(\tau)\right) \end{pmatrix}, \tag{35}$$

where the first component corresponds to (32) and the second to (31). We take the limit $\Delta\tau \to 0$ and with a Taylor series approximation to first order, we obtain the differential equation

$$\frac{d\mathbf{r}(\tau)}{d\tau} = \hat{M}(\tau)\mathbf{r}(\tau), \tag{36}$$

with a matrix operator containing the potential

$$\hat{M}(\tau) = \begin{pmatrix} 0 & V(\tau) - E \\ 1 & 0 \end{pmatrix}. \tag{37}$$

The general solution of this linear nonautonomous system is given by a series of ordered integrals. We must bear in mind that τ is a quasi time that stands for position, so the general solution is a position-ordered exponential in the form

$$\mathbf{r}(\tau) = \hat{R}\,\mathbf{r}_0, \quad \hat{R} \equiv \exp : \int \hat{\mathbf{M}}(\tau) : = \mathbb{I} + \sum_{n=1}^{\infty} \int_{\tau_0}^{\tau} d\tau_1 \int_{\tau_0}^{\tau_1} d\tau_2 \cdots \int_{\tau_0}^{\tau_{n-1}} d\tau_n \hat{M}(\tau_1)\hat{M}(\tau_2)\cdots\hat{M}(\tau_n). \tag{38}$$

In scattering problems, $\mathbf{r}_0 = \mathbf{r}(\tau_0)$ is a vector with plane waves as components; $A(\tau)$ and $\alpha(\tau)$ are set by causal conditions of reflection and transmission. In the case of bound states $\mathbf{r}(\tau_0) \to \mathbf{0}$ when $\tau_0 \to \pm\infty$, which happens only for some values of E substituted in $\hat{M}(\tau)$. The general solution can be simplified by performing the product of matrices[iii]:

$$\hat{R}(\tau) = \begin{pmatrix} \sum\limits_{n\,\mathrm{even}} \int D\tau \prod\limits_{k=1}^{n/2} f_{2k-1} & \sum\limits_{n\,\mathrm{odd}} \int D\tau \prod\limits_{k=1}^{(n-1)/2} f_{2k-1} \\ \sum\limits_{n\,\mathrm{odd}} \int D\tau \prod\limits_{k=1}^{(n-1)/2} f_{2k} & \sum\limits_{n\,\mathrm{even}} \int D\tau \prod\limits_{k=1}^{n/2} f_{2k} \end{pmatrix}, \tag{39}$$

where

$$\mathbf{r} = \hat{R}\,\mathbf{r}_0, \quad f_n = V(\tau_n) - E, \tag{40}$$

and in Feynman's style we have

$$\int D\tau = \int_{\tau_0}^{\tau} d\tau_n \int_{\tau_0}^{\tau_n} d\tau_{n-1} \int_{\tau_0}^{\tau_{n-1}} d\tau_{n-2} \cdots \int_{\tau_0}^{\tau_2} d\tau_1. \tag{41}$$

The lower matrix elements of $\hat{R}$ in the asymptotic limit define the behavior of the wave; it is therefore important to name such functions and, in particular, the modulus of their joint contribution. We define the *spectral function* $\mathcal{F}$ in full analogy with the special functions of the previous cases, as the limits

$$\mathcal{F}(E) = \lim_{\tau\to\pm\infty} \left| \sum_{n\,\mathrm{odd}} \int D\tau \prod_{k=1}^{(n-1)/2} f_{2k} \right| + \lim_{\tau\to\pm\infty} \left| \sum_{n\,\mathrm{even}} \int D\tau \prod_{k=1}^{n/2} f_{2k} \right|. \tag{42}$$

It is important to note that the boundary conditions for bound states imply a vanishing $\mathcal{F}$. These conditions correspond to the evolution of the wave function along x. Meanwhile, the conditions in the upper row of $\hat{R}$, corresponding to the evolution of the derivative, are automatically satisfied due to the Prüfer analysis criterion in Sobolev-type functions (in other words, they are redundant). The function (42) defines the quantized spectral parameters of the system through the transcendental equation

$$\mathcal{F}(E_n) = 0,\ n = 0, 1, ..., n_{\max}. \tag{43}$$

This expression involves all the possibilities of exactly solvable problems for bound states. For the GPE this generalizes the concept of eigenvalues to quantized spectral parameters. The set of solutions E_n is listed here as discrete, but it is well-known that some pathological potentials can exhibit mixed behavior [45], such as bound states in the continuum. This shall be explored elsewhere.

4.2. Non linear case

We address the problem of bound states. In the interstitial region, Eq.(26) is

$$\frac{d^2\phi(\tau)}{d\tau^2} = g\phi^3(\tau) - E\phi(\tau), \tag{44}$$

with $\phi(\tau)$ real and bounded, and $E < 0$. The solution for this equation is $\phi(\tau) = A\,\mathrm{sn}(k\tau - \alpha; m)$. Similarly to the linear case, the boundary conditions are

$$A_{i+1}\mathrm{sn}(k_{i+1}\tau - \alpha_{i+1}; m_{i+1}) = A_i\mathrm{sn}(k_i\tau - \alpha_i; m_i), \tag{45}$$

$$\begin{aligned} A_{i+1}k_{i+1}\mathrm{cn}(k_{i+1}\tau - \alpha_{i+1}; m_{i+1})\mathrm{dn}(k_{i+1}\tau - \alpha_{i+1}; m_{i+1}) &= A_i k_i \mathrm{cn}(k_i\tau - \alpha_i; m_i)\mathrm{dn}(k_i\tau - \alpha_i; m_i) \\ &\quad + V_i\Delta\tau A_i \mathrm{sn}(k_i\tau - \alpha_i; m_i). \end{aligned} \tag{46}$$

We apply the continuous limit again, with the aim of writing a closed differential equation,

$$A(\tau+\Delta\tau)\mathrm{sn}[\mathrm{k}(\tau+\Delta\tau)\tau-\alpha(\tau+\Delta\tau);m(\tau+\Delta\tau)]=A(\tau)\mathrm{sn}[\mathrm{k}(\tau)\tau-\alpha(\tau);m(\tau)], \tag{47}$$

$$\begin{aligned}A(\tau+\Delta\tau)k(\tau+\Delta\tau)\mathrm{cn}[\mathrm{k}(\tau+\Delta\tau)\tau-\alpha(\tau+\Delta\tau);m(\tau+\Delta\tau)]\mathrm{dn}[\mathrm{k}(\tau+\Delta\tau)\tau-\alpha(\tau+\Delta\tau)m(\tau+\Delta\tau)]\\ =A(\tau)k(\tau)\mathrm{cn}[\mathrm{k}(\tau)\tau-\alpha(\tau);m(\tau)]\mathrm{dn}[\mathrm{k}(\tau)\tau-\alpha(\tau);m(\tau)]+V(\tau)\Delta\tau A(\tau)\mathrm{sn}[\mathrm{k}(\tau)\tau-\alpha(\tau);m(\tau)].\end{aligned} \tag{48}$$

Following similar steps that led to (36) from (35), the matching conditions (47) and (48) can be Taylor-expanded to first order in $\Delta\tau$ and thus establish an ordinary differential equation; we show the details in Appendix 4.2.. Therefore, we obtain

$$\frac{d\mathbf{r}(\tau)}{d\tau}=\hat{M}_g(\tau)\mathbf{r}(\tau), \tag{49}$$

with

$$\hat{M}_g(\tau)=\begin{pmatrix}0 & 1\\ V(\tau)-E+g\psi^2(\tau) & 0\end{pmatrix},\qquad \mathbf{r}(\tau)=\begin{pmatrix}\psi(\tau)\\ \varphi(\tau)\end{pmatrix}, \tag{50}$$

and

$$\psi(\tau)=A(\tau)\mathrm{sn}[k(\tau)\tau-\alpha(\tau);m(\tau)],\ \varphi(\tau)=A(\tau)k(\tau)\mathrm{cn}[k(\tau)\tau-\alpha(\tau);m(\tau)]\mathrm{dn}[k(\tau)\tau-\alpha(\tau);m(\tau)]. \tag{51}$$

In two-component form, this equation is rewritten as a linear term and a source term

$$\frac{d}{d\tau}\begin{pmatrix}\psi(\tau)\\ \varphi(\tau)\end{pmatrix}-\begin{pmatrix}0 & 1\\ V(\tau)-E & 0\end{pmatrix}\begin{pmatrix}\psi(\tau)\\ \varphi(\tau)\end{pmatrix}=g\psi^2\begin{pmatrix}0 & 0\\ 1 & 0\end{pmatrix}\begin{pmatrix}\psi(\tau)\\ \varphi(\tau)\end{pmatrix}. \tag{52}$$

We use the following ordered exponential that takes care of the linear part

$$\hat{R}_0=\hat{R}_0(\tau)=\exp\left[:\int\begin{pmatrix}0 & 1\\ V(\tau)-E & 0\end{pmatrix}d\tau\ :\right], \tag{53}$$

$$\frac{d}{d\tau}\hat{R}_0{}^{-1}=-\hat{R}_0{}^{-1}\begin{pmatrix}0 & 1\\ V(\tau)-E & 0\end{pmatrix}. \tag{54}$$

This is done in order to simplify the expressions in (52) such that

$$\hat{R}_0\frac{d}{d\tau}\left(\hat{R}_0{}^{-1}\begin{pmatrix}\psi(\tau)\\ \varphi(\tau)\end{pmatrix}\right)=\frac{d}{d\tau}\begin{pmatrix}\psi(\tau)\\ \varphi(\tau)\end{pmatrix}-\begin{pmatrix}0 & 1\\ V(\tau)-E & 0\end{pmatrix}\begin{pmatrix}\psi(\tau)\\ \varphi(\tau)\end{pmatrix}. \tag{55}$$

Then our system resembles an *interaction picture*, where the nonlinearity acts like the source or perturbation:

$$\hat{R}_0\frac{d}{d\tau}\left(\hat{R}_0{}^{-1}\begin{pmatrix}\psi(\tau)\\ \varphi(\tau)\end{pmatrix}\right)=g\psi^2\begin{pmatrix}0 & 0\\ 1 & 0\end{pmatrix}\begin{pmatrix}\psi(\tau)\\ \varphi(\tau)\end{pmatrix}. \tag{56}$$

Left-multiplication by $\hat{R}_0$ and a redefinition of the spinor leads to the simplified system:

$$\frac{d}{d\tau}\begin{pmatrix}\tilde{\psi}\\ \tilde{\varphi}\end{pmatrix}=g\psi^2\tilde{\sigma}_-\begin{pmatrix}\tilde{\psi}\\ \tilde{\varphi}\end{pmatrix},\ \begin{pmatrix}\tilde{\psi}\\ \tilde{\varphi}\end{pmatrix}=\hat{R}_0{}^{-1}\begin{pmatrix}\psi\\ \varphi\end{pmatrix},\qquad \tilde{\sigma}_-=\hat{R}_0{}^{-1}\begin{pmatrix}0 & 0\\ 1 & 0\end{pmatrix}\hat{R}_0. \tag{57}$$

Both sides can be integrated in order to build an iterative integral series for a small time step $\Delta\tau$

$$\begin{pmatrix}\tilde{\psi}\\ \tilde{\varphi}\end{pmatrix}_{\Delta\tau}-\begin{pmatrix}\tilde{\psi}\\ \tilde{\varphi}\end{pmatrix}_0=\int_0^{\Delta\tau}g\psi^2\tilde{\sigma}_-\begin{pmatrix}\tilde{\psi}\\ \tilde{\varphi}\end{pmatrix}d\tau=\Delta\tau g\psi^2(0)\tilde{\sigma}_-(0)\begin{pmatrix}\tilde{\psi}(0)\\ \tilde{\varphi}(0)\end{pmatrix}+O_2(\Delta\tau) \tag{58}$$

$$=\Delta\tau g\psi^2(0)\begin{pmatrix}0 & 0\\ 1 & 0\end{pmatrix}\begin{pmatrix}\psi(0)\\ \varphi(0)\end{pmatrix}+O_2(\Delta\tau). \tag{59}$$

Without approximations we note that

$$\exp\left(\Delta\tau g\psi^2(0)\begin{pmatrix}0 & 0\\ 1 & 0\end{pmatrix}\right)=\mathbb{I}+\Delta\tau g\psi^2(0)\begin{pmatrix}0 & 0\\ 1 & 0\end{pmatrix}, \tag{60}$$

which allows to write (59) as

$$\begin{pmatrix}\tilde{\psi}\\ \tilde{\varphi}\end{pmatrix}_{\Delta\tau} \simeq \left(\mathbb{I}+\Delta\tau g\psi^2(0)\begin{pmatrix}0&0\\1&0\end{pmatrix}\right)\begin{pmatrix}\psi(0)\\ \varphi(0)\end{pmatrix} \simeq \exp\left(\Delta\tau g\psi^2(0)\begin{pmatrix}0&0\\1&0\end{pmatrix}\right)\begin{pmatrix}\psi(0)\\ \varphi(0)\end{pmatrix}, \tag{61}$$

accurate to order 2, and our small-step solution reads

$$\begin{pmatrix}\psi\\ \varphi\end{pmatrix}_{\Delta\tau} \simeq \hat{R}_0\exp\left(\Delta\tau g\psi^2(0)\begin{pmatrix}0&0\\1&0\end{pmatrix}\right)\begin{pmatrix}\psi(0)\\ \varphi(0)\end{pmatrix}. \tag{62}$$

It is advantageous to view this solution as a composition of two exponential maps corresponding to linear and nonlinear contributions. In general, the successive composition for infinitesimal time steps is the following ordered product

$$\begin{aligned}\begin{pmatrix}\psi_n\\ \varphi_n\end{pmatrix}_{\tau} \simeq{}& \hat{R}_0(n,n-1)\exp\left(\Delta\tau g\psi_{n-1}^2\begin{pmatrix}0&0\\1&0\end{pmatrix}\right)\hat{R}_0(n-1,n-2)\exp\left(\Delta\tau g\psi_{n-2}^2\begin{pmatrix}0&0\\1&0\end{pmatrix}\right)\\ &\times\cdots\cdots\hat{R}_0(1,0)\exp\left(\Delta\tau g\psi_0^2\begin{pmatrix}0&0\\1&0\end{pmatrix}\right)\begin{pmatrix}\psi(0)\\ \varphi(0)\end{pmatrix}.\end{aligned} \tag{63}$$

Finally, we apply the limit when $n\to\infty$, $\Delta\tau\to 0$ but τ finite. This leads to the familiar form of the *Trotter limit* [46][iv] for which the product of exponentials can be expressed as a single exponential map:

$$\hat{R}=\lim_{n\to\infty}\prod_{j=1}^{n}\hat{R}_0(j,j-1)e^{g\tau\sigma_-\psi_{n-1}^2/n}. \tag{64}$$

The instructions to utilize this formula for exact solutions to any desired order are iterative: First build $\hat{R}$ for a given n, say $n=1$, and apply it to the spinor $\Psi_1=(\psi_1,\varphi_1)^{\mathrm{T}}$. Then, substitute $n=2$ in $\hat{R}$ and apply it to get $\Psi_2=(\psi_2,\varphi_2)^{\mathrm{T}}$, and so on. The last function gives rise to a closed expression for $\hat{R}$ as in (64), whose elements are set as

$$\mathcal{F}_g(E)=\lim_{\tau\to\pm\infty}\left[|\hat{R}_{21}|+|\hat{R}_{22}|\right], \tag{65}$$

and this is our spectral function for nonlinear problems $\mathcal{F}_g(E)=0$, whose roots yield the required solutions.

5. Remarks on classical and quantum integrability

As announced in the previous section, exact solutions require integrability conditions that can be stated in terms of phase-space variables. It is crucial to provide a broad analysis in this context. It is clear that classical and quantum-mechanical equations of motion yield different results for general potentials beyond harmonic approximations. Concretely, the quantum and classical cases differ in the solvability criteria: In one scenario, Newton's 2nd law is solved for canonical variables of the dynamical system and, in the other case, the wave equation is solved for a complex amplitude. However, the Heisenberg picture produces the same Hamilton equations, but now for operators; if there are not enough separation constants, neither classical nor quantum cases can be solved (*e.g.* by quadratures, but quantum-mechanically translates into a deficiency of conserved compatible operators). So even if the classical case allows solvability by quadratures –here the 1D system with conserved energy H guarantees solutions by integrals– we are left with a stationary wave equation that itself represents a non-trivial classical dynamical system, such as (36) and its nonlinear version (49) analyzed throughout the present paper.

To show that this system is a nontrivial one, let us start with the stationary wave equation and build the dynamical system $x\to t$, $\psi(x)\to X(t)$, $\psi'(x)\to\dot{X}(t)=P(t)$ with the following nonautonomous form

$$\frac{d}{dt}\begin{pmatrix}X\\ P\end{pmatrix}=\begin{pmatrix}0&1\\ E-V(t)&0\end{pmatrix}\begin{pmatrix}X\\ P\end{pmatrix}. \tag{66}$$

The energy $U=\frac{1}{2}(P^2+[E-V(t)]\,X^2)$ is no longer conserved, so for arbitrary $V(t)$ this is, in general, a nonintegrable system in the classical sense, despite being a quantum system with conserved H^{system}. It can present nonlinear phenomena such as dynamical localization and chaos (also classical). The energy U gives rise to the very famous Hill equation [47] when it is perturbed, and it is the subject of various stability studies when such small perturbation has the form $V(t)=V_0(t)+\delta V(t)$, based on specific behaviors of the corresponding solutions for $V_0(t)$ (see stability gaps or Arnold tongues [48, 49]). There is a finite list of V_0 that are considered as solvable. Indeed, δV can produce highly nontrivial effects, *e.g.* chaos, and requires the explicit evaluation of the spectral function $\mathcal{F}(E)$. So even though the GP equation has been formally solved for all possible potentials in

this paper,

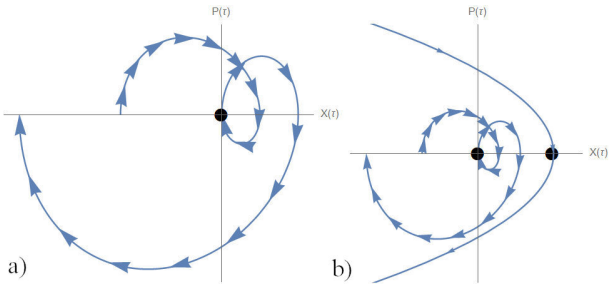

FIGURE 12. a): Linear stable equilibrium. b): Nonlinear stable and unstable equilibria. When $\gamma < 0$, the bright solitons (only bound states) correspond to a critical point $(X(\tau) = 0, P(\tau) = 0)$ in phase space. When $g > 0$, we have dark solitons (unbounded). These correspond to points away from the origin, *i.e.*, $\left(X(\tau) = \pm\sqrt{(E - V(\tau))/g}, P(\tau) = 0\right)$.

the evaluation of $\mathcal{F}$ involves a high degree of complexity and some interesting surprises might await for us.

Regards nonlinearities $V \to V + g|X|^2$, we have showed by construction that, indeed, it is possible to obtain a formal expression for waves and spectral functions that solve the problem. Two observations are in order:

a) It is expected that every Liouville flow will solve any Hamiltonian dynamical system (formal solution) but that does not mean that the expression is easy to evaluate for energies E that satisfy the boundary condition $X(t) \to X_\infty$, $t \to \pm\infty$.

b) Quantum nonintegrability implies the classical one at the level of the equations followed by observables. However, quantum integrability seen as a complete set of compatible and conserved observables does not ensure analytically solvable wave equations. For this reason, there are some reservations when defining the concept of quantum chaos, and we work within more modest limits. A distinction proposed by Berry [50], "chaos" versus "chaology", deals with chaotic wave-like systems conceived as those whose classical limit yields a system that presents mixing, ergodicity and sensitivity to initial conditions.

A phase space diagram comparing the two cases $g \neq 0$ and $g = 0$ is provided in Fig. 12. The construction is explained in Appendix B.

6. Analytical and numerical examples

Now that the general method of solution by layers has been formulated, we are ready to compute spectral parameters and wave functions for any potential of interest. In particular, the harmonic oscillator trap is a typical example with frequent occurrence in experimental setups, and has been addressed only with numerical means. Also, by comparison, we compute numerically the wave functions of the square well in order to find the (negligible) deviations from our analytical method.

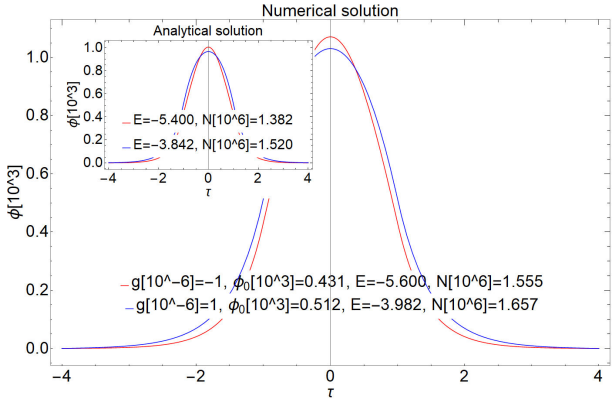

FIGURE 13. Numerical ground state for both coupling cases. The large curves are computed by shooting+Runge-Kutta of 4th order+bisection. The inset contains the analytical solution.

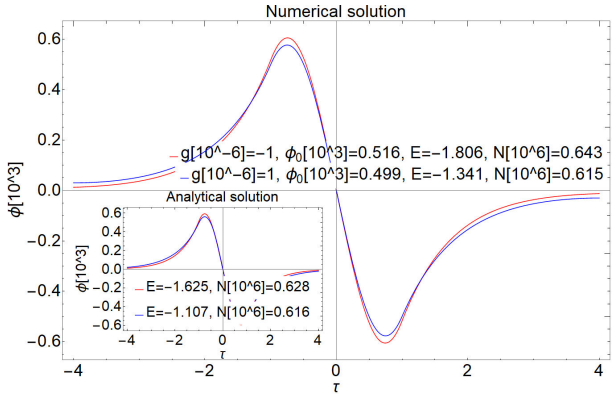

FIGURE 14. First excited state for both couplings. As before, Fig. "13, the numerical solution is given by shooting+Runge-Kutta of 4th order+bisection.

6.1. Square well potential

A Runge-Kutta method of 4 point quadrature is implemented, together with a shooting method for the boundary conditions (wave functions and derivatives) and a bisection routine (for energies). This long numerical method is compared with the efficiency of our graphical method described in Sec. 3.2. In Figs. 9 and 10 we gave special parameters for the ground and the first excited state, respectively. Now, in Figs. 13 and 14 we provide the numerical results with excellent agreement, both in shape (wave function) and energy values. Both methods take as initial condition $\phi(\tau = -4) = 5 \times 10^{-9}$ for the ground state (not zero, avoiding the trivial fixed point) in a well of width $2\tau_0 = 2$ and depth $V_0 = 6$, obtaining energies with a relative error $\Delta E = |E_{\rm num} - E_{\rm ana}|/|E_{\rm ana}| = 0.035$ for $g[10^{-6}] = 1$ and 0.037 for $g[10^{-6}] = -1$. The same exercise can be done for the excited state. Given the scaling properties of the potential $g|\phi|^2$, we have chosen in this example an order of magnitude $N \sim 10^6$, comparable with a realistic number of particles in a BEC. The value of the coupling scales inversely, *i.e.*, $g \sim 10^{-6}$. It is easy to modify

this value to other situations where the number of atoms can reach 10^9 (a current record).

6.2. Harmonic oscillator potential

As in the previous case, we give a comparison between two methods. The harmonic oscillator cannot be solved in closed form for GPE, but can be approximated arbitrarily well by our layered method. The specifications are given in the following sections.

6.2.1. *Nonlinear recurrence vs traditional numerical method*

We work with a potential $V(\tau) = 0.5\tau^2$, corresponding to a frequency $\omega = \sqrt{2}$ as the mass is $1/2$. The full wave function is constructed by means of the recurrence (47) and (48) starting from a initial amplitude at the rightmost point and propagating to the left (retropropagation). The initial amplitude is $A(\tau = 2) = 10^{-1}$, the phase $\alpha(\tau = 2) = -0.29\pi$ and interstitial step $\Delta\tau = 0.001$. The results for the ground state and the first excited state are shown in Figs. 15 and 16. Meanwhile, for the first excited state we start from $A(\tau = 2) = 10^{-1}$, $\alpha(\tau = 2) = -0.55\pi$ and the same $\Delta\tau$. In both figures we observe an important shift in the energy as a function of g and N. It is important to note that for a fixed g and N, the energies are quantized and, in principle, form

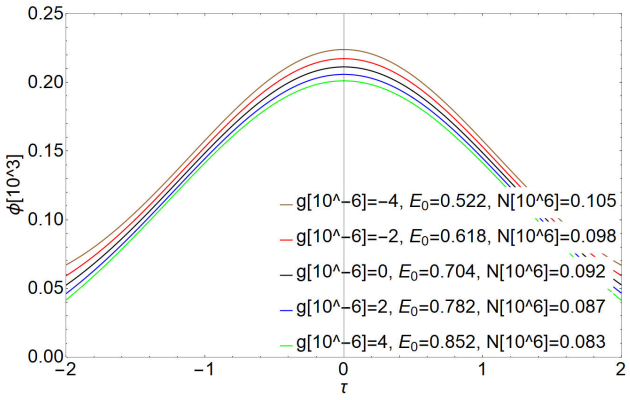

FIGURE 15. Ground state for different couplings. The curvatures display qualitatively different features.

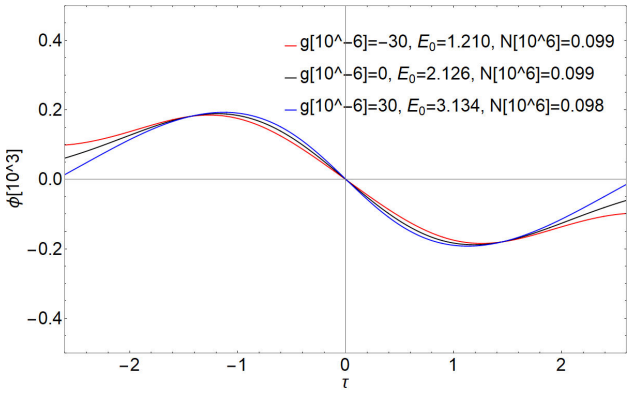

FIGURE 16. First excited state for three coupling cases. The curvature and localization width of the wave vary accordingly.

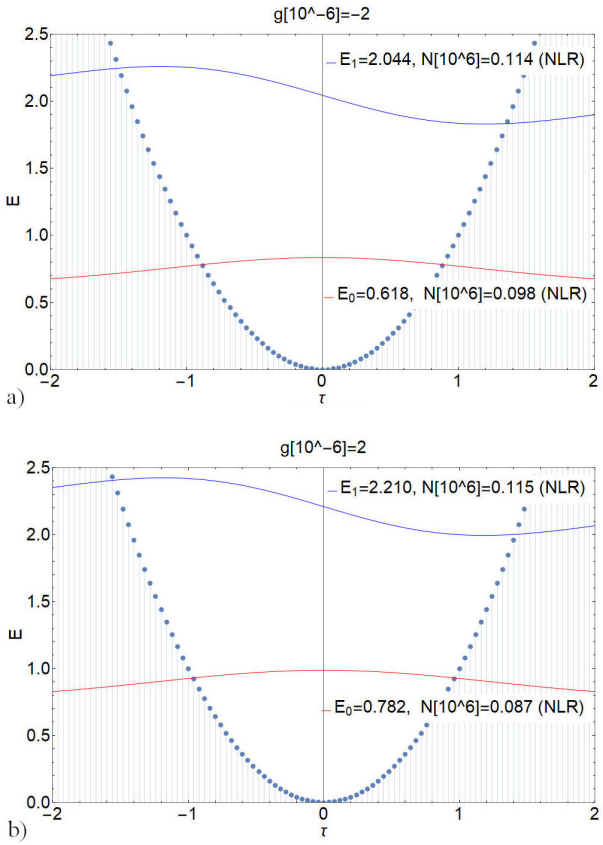

FIGURE 17. Results from the nonlinear recurrence. a): $g < 0$. b): $g > 0$. For approximately the same number or particles, the energies are shifted.

an infinite ladder. In our evaluation we restrict ourselves to a finite interval, thus producing only the first two levels. These results must be compared with the RK4+shooting+bisection method.

The results in Figs. 17 and 18 are found under the following conditions: a) *Ground state:* initial condition $\phi(-2) = 0.0592$, relative error in energy $\Delta E = 0.001$ and relative error in particle number $\Delta N = 0$ for $g = -2$ (good agreement); for $g = +2$ the condition is $\phi(-2) = 0.0462$ with relative errors $\Delta E = 0$ and $\Delta N = 0$ (excellent agreement to three decimal places). b) *First excited state:* initial condition $\phi(-2.6) = 0.0732$ and relative errors $\Delta E = 0.0004$ and $\Delta N = 0$ for $g = -2$; meanwhile, for $g = +2$, we have $\phi(-2.6) = 0.0646$, $\Delta E = 0$ and $\Delta N = 0$.

6.3. Discussion of results

For the paradigmatic case of the oscillator trap, we can compare the efficiency and accuracy of our new recurrence. A good agreement is found (three decimal places) between the spectral parameters and particle numbers for various values of g. Although, g and N are independent parameters, when a solution is found for a specific energy, the value of N must

be calculated using the normalization integral. As to the wave functions, the shapes are surprisingly similar, as displayed in

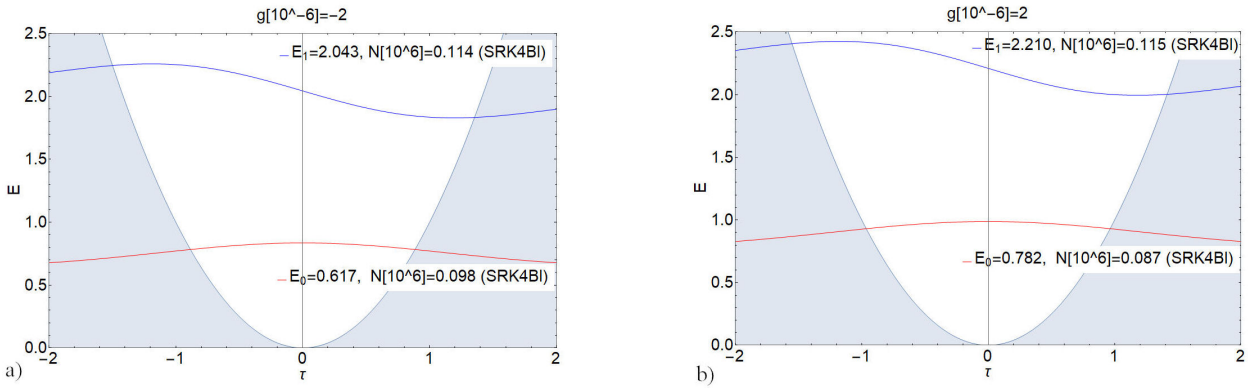

FIGURE 18. Results from RK4+shooting+bisection. Similar results as in Fig. 17.

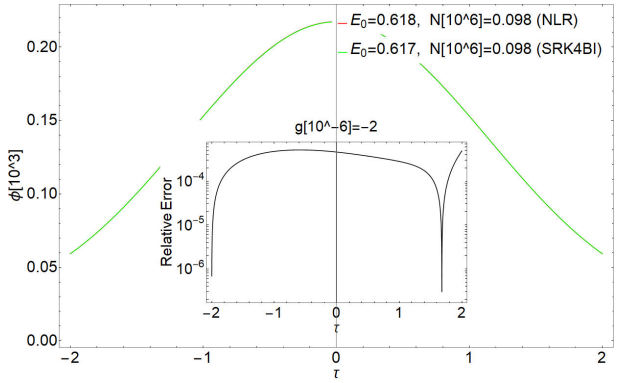

FIGURE 19. Ground state for negative nonlinear coupling and relative error between RK4+shooting+bisection and nonlinear recurrence. The differences are indistinguishable.

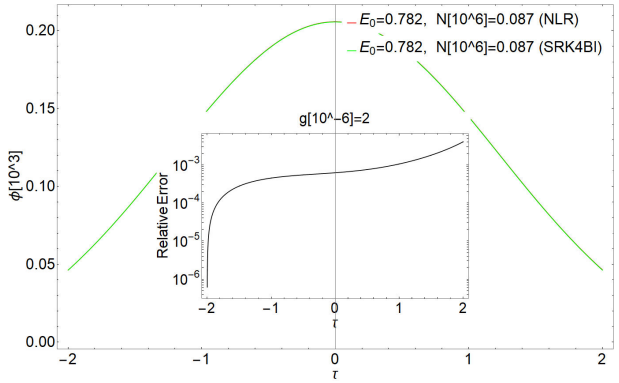

FIGURE 20. Ground state for positive nonlinear coupling and relative errors. The same comments as in Fig. 19 apply.

the insets of Figs. 19, 20, 21 and 22, where very small relative errors are reported.

6.3.1. A connection with BECs

Along this paper we have assumed that all solutions represent stable configurations of an atomic ultracold gas, so it is important to put our results into context. In Ref. [51] the authors show that couplings can be tuned via Feshbach resonance in order to produce negative interaction energies and bright

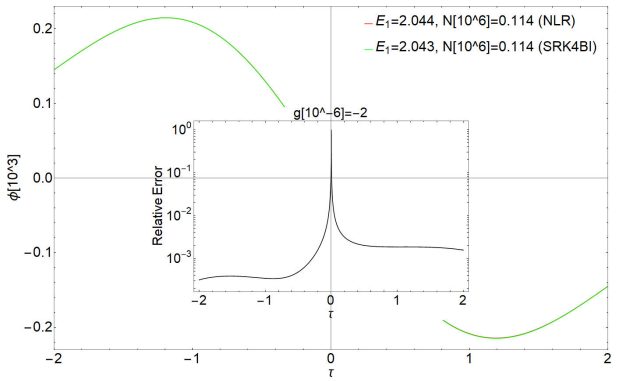

FIGURE 21. First excited state for negative nonlinear coupling. The curves are identical, but the relative error spikes around $\tau = 0$ as the wave function vanishes.

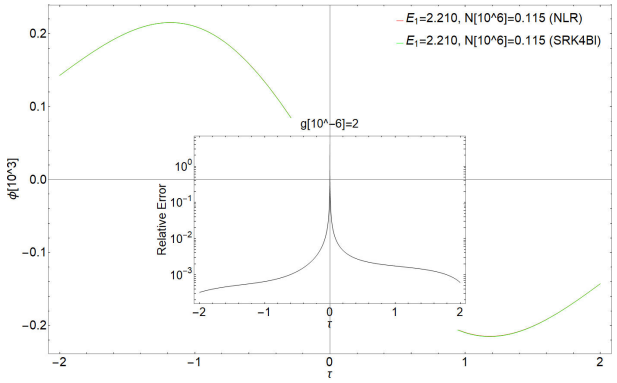

FIGURE 22. First excited state for positive nonlinear coupling. Same comments as in Fig. 21 apply.

solitons after a BEC of ^{7}Li has been formed. Indeed, the condensate has a finite lifetime, which is large compared with the period of an elongated harmonic trap. The literature also reports ^{23}Na, with scattering length $a = 2.75$ nm in traps of an aspect ratio of roughly 1:10. It is important to note that

both strong and weak regimes of the coupling constant can be achieved [37–40]

On experimental grounds, excited states of condensates in traps have been probed and measured in [52, 53]. To this effect it is required that once the BEC is formed all the particles belong to the same state, *e.g.* the excited state of a trap or potential well. Our spectral parameter (not an eigenvalue) follows a rigorously derived quantization condition, but one comment is in order: the allowed values are determined by the potential parameters *and the wave amplitude*, therefore a variation of N shifts the energies continuously. Once N is fixed, what the linear and nonlinear solutions share in common is the number of nodes, parameterized by n in our discussion.

It should be noted that stability analyses *à la* Bogoliubov of the GPE abound in the literature. A very detailed study is given in [54]. For scattering states this analysis was carried out in [16]. In most cases it boils down to a reality condition for the square root that determines the energy as a function of the wave number and the nonlinear coupling constant g, *i.e.*, $k = \sqrt{E - g\psi^2}$.

As to the broad applicability of our method, it is convenient to compare convergence and accuracy for potentials with untamed oscillations and waves with nontrivial interference effects. The traditional RK4 is not better suited in such cases, due to a poor estimate of quadratures. We expect our layer method to perform better in situations of interest, such as Anderson localization of BECs [55], but in a strong coupling regime [56].

7. Conclusions

In this work we have solved two paradigmatic problems of bound states for the nonlinear Schrödinger equation: a defect in the form of a Dirac delta (both negative and, surprisingly, positive with an attractive nonlinear interaction) and the square well potential. The equation that determines the allowed energies is solved using an improved graphical method for the GP equation, not reported in the literature. Then, we used the layered construction made of Dirac combs to show that the solution method for bound states is also effective for the nonlinear case. In this way, we approached the 1D equation with a general potential. In the continuous limit, a generalization of the Mello and Kumar equation[vi] was found and we showed that the nonlinear form of these equations is identical to a mapping of the Gross-Pitaevskii equation to phase space. We also showed that any stationary Schrödinger equation, both linear and nonlinear, has formal solutions given by a series of ordered exponentials in the position variable; so technically any problem is solvable, not just the harmonic oscillator. We may conclude, from our discussions, that the complexity of the general problem resides in the spectral equations $\mathcal{F}(E) = 0$, where $\mathcal{F}$ is expressed as a limit. To find the corresponding roots will sometimes require numerical techniques of evaluation, as the ordered series may not have a recognizable form. However, we note that, by construction, the wave functions are closed expressions for any potential and this settles the issue of exact solvability for 1D integrable quantum mechanical systems. In the last section we gave a comparison between our technique and other methods, mainly numerical, available in the literature. This gave us the opportunity of providing a clear connection with dimensional reductions together with experimental parameters for potential applications.

Appendix

A. Deduction of equations for the nonlinear case

The Jacobi elliptic function $\phi_i(\tau) = A_i \mathrm{sn}(k_i\tau - \alpha_i; m_i)$ satisfies the differential equation

$$\frac{d^2\phi_i(\tau)}{d\tau^2} = \frac{2m_i^2k_i^2}{A_i^2}\phi_i^3(\tau) - k_i^2(1+m_i^2)\phi_i(\tau). \tag{A.1}$$

If we compare the Eqs. (44) and (A.1), we obtain $(2m_i^2k_i^2/A_i^2) = g$ and $E = k_i^2(1+m_i^2)$, *i.e.*, $(2m^2(\tau)k^2(\tau)/A^2(\tau)) = g$ and $E = k^2(\tau)(1+m^2(\tau))$.

We expand the Eqs. (47) and (48) to first order in $\Delta\tau$, and retain the derivatives, which give the following answers:

$$\frac{d}{d\tau}\left[A(\tau)\mathrm{sn}\left(k(\tau)\tau - \alpha(\tau); m(\tau)\right)\right] = k(\tau)A(\tau)\mathrm{cn}\left(k(\tau)\tau - \alpha(\tau); m(\tau)\right)\mathrm{dn}\left(k(\tau)\tau - \alpha(\tau); m(\tau)\right), \tag{A.2}$$

$$\frac{d}{d\tau}\left[k(\tau)A(\tau)\mathrm{cn}\left(k(\tau)\tau - \alpha(\tau); m(\tau)\right)\mathrm{dn}\left(k(\tau)\tau - \alpha(\tau); m(\tau)\right)\right] = k^2(\tau)A(\tau)\mathrm{sn}\left(k(\tau)\tau - \alpha(\tau); m(\tau)\right)$$
$$\times\left[2m^2(\tau)\mathrm{sn}^2\left(k(\tau)\tau - \alpha(\tau); m(\tau)\right) - (1+m^2(\tau))\right]. \tag{A.3}$$

We define the wave functions as

$$\psi(\tau) = A(\tau)\mathrm{sn}[k(\tau)\tau - \alpha(\tau); m(\tau)], \tag{A.4}$$

$$\varphi(\tau) = A(\tau)k(\tau)\mathrm{cn}[k(\tau)\tau - \alpha(\tau); m(\tau)]\mathrm{dn}[k(\tau)\tau - \alpha(\tau); m(\tau)], \tag{A.5}$$

such that

$$\frac{d}{d\tau}\begin{pmatrix}\psi(\tau)\\ \varphi(\tau)\end{pmatrix} = \begin{pmatrix}0 & 1\\ V(\tau) - k^2(\tau)(1+m^2(\tau)) + \frac{2m^2(\tau)k^2(\tau)}{A^2(\tau)}\psi^2(\tau) & 0\end{pmatrix}\begin{pmatrix}\psi(\tau)\\ \varphi(\tau)\end{pmatrix}.$$

Then, we obtain Eq. (B.1).

B. Evolution in phase-space and critical points for the nonlinear problem

In the nonlinear case, we consider a first order nonlinear spinor differential equation.

$$\frac{d}{d\tau}\begin{pmatrix}\psi(\tau)\\ \varphi(\tau)\end{pmatrix} = \begin{pmatrix}0 & 1\\ V(\tau) - E + g\psi^2(\tau) & 0\end{pmatrix}\begin{pmatrix}\psi(\tau)\\ \varphi(\tau)\end{pmatrix}. \tag{B.1}$$

If we want to analyze this system in phase space, we must define $X(\tau) = \psi(\tau)$ and $P(\tau) = \varphi(\tau)$. The resulting nonautonomous system evolves in time with the possibility of self-intersecting trajectories in (X, P). The critical points are such that $dX(\tau)/d\tau = 0$ and $dP(\tau)/d\tau = 0$, and define the existence of bright and dark solitons. Then $P(\tau) = 0$ and $(V(\tau) - E)X(\tau) + gX^2(\tau) = 0$. For the linear case, the only critical point is $(X(\tau) = 0, P(\tau) = 0)$ and this corresponds to the bound state. In the general case, the critical point $(X(\tau) = 0, P(\tau) = 0)$ is the bright soliton with $g < 0$; moreover, the points $\left(X(\tau) = \pm\sqrt{(E - V(\tau))/g}, P(\tau) = 0\right)$ are the dark solitons with $g > 0$, see Fig. 12.

Acknowledgments

Financial support from CONAHCYT under Grant No. CF-2023-G-763 is acknowledged. M.M. is grateful to VIEP-BUAP for support under Project No. 100518931-BUAP-CA-289.

$i.$(Parameter). For condensates, $E = \mu$ is the chemical potential whenever $\int \rho(x)d^3x = \mathcal{N}$ is normalized to particle number $\mathcal{N}$. Note the change in normalization for 1D by a factor, *i.e.*, $\int |\phi(x)|^2 dx = N \propto \mathcal{N}$ [41].

$ii.$ The use of an effective coupling constant in the dimensional reduction covers both weakly and strongly interacting cases. In [41] it was argued that $g = g_{1\mathrm{D}} = 3g_{3\mathrm{D}}/(4\pi a_\perp^2\sqrt{2a\mathcal{N}})$ is more suitable in the strong regime.

$iii.$ The sums resemble a Dyson series. The first term is defined as 1 for the diagonal entries of $\hat{R}$ and 0 for off-diagonal elements.

$iv.$ Sometimes also associated to Glauber, although the name Zassenhaus is mentioned more often when the Baker-Campbell-Hausdorff series terminates.

$v.$(system). We highlight here that an effectively two-dimensional system without integrals of motion (X and t are two dimensions) does not predict the existence of solutions by separability, which makes the concept of quantum solvability and integrability more demanding.

$vi.$ In the context of transport theory, this is known as Dorokhov-Mello-Pereyra-Kumar (DMPK) equation.

1. L. Infeld and T. E. Hull, The Factorization Method, *Rev. Mod. Phys.* **23** (1951) 21, https://link.aps.org/doi/10.1103/RevModPhys.23.21

2. F. Dalfovo *et al.*, Theory of Bose-Einstein condensation in trapped gases, *Rev. Mod. Phys.* **71** (1999) 463, https://link.aps.org/doi/10.1103/RevModPhys.71.463

3. A. Griffin, D. Snoke, and S. Stringari, Bose-Einstein Condensation, 1st edition (Cambridge University Press, New York, 1995), pp. 13-462, https://books.google.com.mx/books?id=suqJdr2pPIsC

4. K. Frye *et al.*, The Bose-Einstein Condensate and Cold Atom Laboratory, *EPJ Quantum Technology* **8** (2021), https://doi.org/10.1140/epjqt/s40507-020-00090-8

5. C. Chin *et al.*, Feshbach resonances in ultracold gases, *Rev. Mod. Phys.* **82** (2010) 1225, https://link.aps.org/doi/10.1103/RevModPhys.82.1225

6. T. Kraemer *et al.*, Optimized production of a cesium Bose - Einstein condensate, *Applied Physics B* **79** (2004), https://doi.org/10.1007/s00340-004-1657-5

7. A. J. Moerdijk, B. J. Verhaar, and A. Axelsson, Resonances in ultracold collisions of ^{6}Li, ^{7}Li, and ^{23}Na, *Phys. Rev. A* **51** (1995) 4852, https://link.aps.org/doi/10.1103/PhysRevA.51.4852

8. C. C. Bradley, C. A. Sackett, and R. G. Hulet, Bose-Einstein Condensation of Lithium: Observation of Limited Condensate Number, *Phys. Rev. Lett.* **78** (1997) 985, https://link.aps.org/doi/10.1103/PhysRevLett.78.985

9. J. L. Roberts *et al*., Magnetic Field Dependence of Ultracold Inelastic Collisions near a Feshbach Resonance, *Phys. Rev. Lett.* **85** (2000) 728, https://link.aps.org/doi/10.1103/PhysRevLett.85.728

10. J. Kerr, A new relation between electricity and light: Dielectrified media birefringent, *The London, Edinburgh, and Dublin Philosophical Magazine and Journal of Science* **50** (1875) 337, https://doi.org/10.1080/14786447508641302

11. J. Kerr, A new relation between electricity and light: Dielectrified media birefringent (Second paper), *The London, Edinburgh, and Dublin Philosophical Magazine and Journal of Science* **50** (1875) 446, https://doi.org/10.1080/14786447508641319

12. F. London and H. London, The Electromagnetic Equations of the Supraconductor, *Proc. A* **149** (1935) 71, https://doi.org/10.1098/rspa.1935.0048

13. P. W. Higgs, Broken Symmetries and the Masses of Gauge Bosons, *Phys. Rev. Lett.* **13** (1964) 508, https://link.aps.org/doi/10.1103/PhysRevLett.13.508

14. J. Goldstone, Field Theories with Superconductor Solutions, *Nuovo Cim.* **19** (1961) 154, https://doi.org/10.1007/BF02812722

15. G. Altarelli and S. Forte, The Standard Model of Electroweak Interactions. In: Schopper, H. (eds) Particle Physics Reference Library, (Springer, Cham, Switzerland, 2020), pp. 35-81, https://doi.org/10.1007/978-3-030-38207-0_3

16. M. Mirón and E. Sadurní, Stationary scattering for the nonlinear Schrödinger equation with point-like obstacles: exact solutions, *Nonlinear Dynamics* **113** (2025) 5627, https://doi.org/10.1007/s11071-024-10448-7

17. I. S. Gradshteyn and I. M. Ryzhik, Table of integrals, series, and products, Seventh ed. (Elsevier/Academic Press, Amsterdam, 2007), pp. 859-873.

18. J. N. Ginocchio, A class of exactly solvable potentials. I. One-dimensional Schrödinger equation, *Annals Phys.* **152** (1984) 203, https://doi.org/10.1016/0003-4916(84)90084-8

19. P. M. Morse, Diatomic Molecules According to the Wave Mechanics. 2. Vibrational Levels, *Phys. Rev.* **34** (1929) 57, https://doi.org/10.1103/PhysRev.34.57

20. C. Eckart, The Penetration of a Potential Barrier by Electrons, *Phys. Rev.* **35** (1930) 1303, https://link.aps.org/doi/10.1103/PhysRev.35.1303

21. G. Poschl and E. Teller, Bemerkungen zur Quantenmechanik des anharmonischen Oszillators, *Z. Phys.* **83** (1933) 143, https://doi.org/10.1007/BF01331132

22. G. Natanzon, Study of the one-dimensional Schroedinger equation generated from the hypergeometric equation, *Vestnik Leningrad. Univ.* **10** (1971) 22 https://doi.org/10.48550/arXiv.physics/9907032

23. F. Cooper, A. Khare, and U. Sukhatme, Supersymmetry and quantum mechanics, *Physics Reports* **251** (1995) 267, https://doi.org/10.1016/0370-1573(94)00080-M

24. A. Mostafazadeh, Real description of classical Hamiltonian dynamics generated by a complex potential, *Physics Letters A* **357** (2006) 177, https://doi.org/10.1016/j.physleta.2006.04.045

25. A. Mostafazadeh, Quantum mechanics of Klein -Gordon-type fields and quantum cosmology, *Annals of Physics* **309** (2004) 1, https://doi.org/10.1016/j.aop.2003.08.010

26. C. Grosche and F. Steiner, Handbook of Feynman Path Integrals, 1st edition. (Springer Berlin, Heidelberg, New York, 1998), pp. 1-122, https://doi.org/10.1007/BFb0109520

27. J. I. Castro-Alatorre, D. Condado, and E. Sadurni, Exact Green's functions for localized irreversible potentials, *Revista Mexicana de Física* **69** (2023) 050401 1 -, https://doi.org/10.31349/revmexfis.69.050401

28. E. Moshinsky, M. Sadurní, A. del Campo, Alternative method for determining the Feynman propagator of a relativistic quantum mechanical problem, *SIGMA* **3** (2007), 110, https://doi.org/10.3842/SIGMA.2007.110

29. P. A. Mello and N. Kumar, Quantum Transport in Mesoscopic Systems: Complexity and Statistical Fluctuations. A Maximum Entropy Viewpoint, (Oxford University Press, New York, 2004), https://doi.org/10.1093/acprof:oso/9780198525820.001.0001

30. I. Bloch, Probing and Controlling Quantum Matter in Crystals of Light, In CLEO:2015 (Optica Publishing Group, New York, 2015) pp. FTh4D.1, https://opg.optica.org/abstract.cfm?URI=CLEO_QELS-2015-FTh4D.1.

31. L. D. Carr, K. W. Mahmud, and W. P. Reinhardt, Tunable tunneling: An application of stationary states of Bose-Einstein condensates in traps of finite depth, *Phys. Rev. A* **64** (2001) 033603, https://link.aps.org/doi/10.1103/PhysRevA.64.033603

32. R. Rajaraman, Solitons and Instantons: An Introduction to Solitons and Instantons in Quantum Field Theory, (North-Holland Publishing Company, North-Holland, 1982), pp. 4-34, https://books.google.com.mx/books?id=1XucQgAACAAJ.

33. W. Bao and H. Wang, An efficient and spectrally accurate numerical method for computing dynamics of rotating Bose -Einstein condensates, *Journal of Computational Physics* **217** (2006) 612, https://doi.org/10.1016/j.jcp.2006.01.020

34. L. M. Symes, R. I. McLachlan, and P. B. Blakie, Efficient and accurate methods for solving the time-dependent spin-1 Gross-Pitaevskii equation, *Phys. Rev. E* **93** (2016) 053309, https://link.aps.org/doi/10.1103/PhysRevE.93.053309

35. W. Bao and F. Y. Lim, Computing Ground States of Spin-1 Bose -Einstein Condensates by the Normalized Gradient Flow, *SIAM Journal on Scientific Computing* **30** (2008) 1925, https://doi.org/10.1137/070698488

36. R. J. LeVeque, Finite Difference Methods for Ordinary and Partial Differential Equations, (SIAM, Philadelphia,

2007), pp. 160-161, https://epubs.siam.org/doi/abs/10.1137/1.9780898717839.

37. K. E. Strecker *et al*., Formation and propagation of matter-wave soliton trains, *Nature* **417** (2002) 150, https://www.nature.com/articles/nature747

38. A. Weller *et al*., Experimental Observation of Oscillating and Interacting Matter Wave Dark Solitons, *Phys. Rev. Lett.* **101** (2008) 130401, https://link.aps.org/doi/10.1103/PhysRevLett.101.130401

39. T. Giamarchi, Quantum Physics in One Dimension (Oxford University Press, New York, 2003), pp. 1-94, https://doi.org/10.1093/acprof:oso/9780198525004.001.0001.

40. E. Haller *et al*., Pinning quantum phase transition for a Luttinger liquid of strongly interacting bosons, *Nature* **466** (2010) 597, https://www.nature.com/articles/nature09259

41. L. Salasnich, A. Parola, and L. Reatto, Effective wave equations for the dynamics of cigar-shaped and disk-shaped Bose condensates, *Phys. Rev. A* **65** (2002) 043614, https://link.aps.org/doi/10.1103/PhysRevA.65.043614

42. A. Görlitz *et al*., Realization of Bose-Einstein Condensates in Lower Dimensions, *Phys. Rev. Lett.* **87** (2001) 130402, https://link.aps.org/doi/10.1103/PhysRevLett.87.130402

43. I. V. Barashenkov, E. V. Zemlyanaya, and M. Bär, Traveling solitons in the parametrically driven nonlinear Schrödinger equation, *Phys. Rev. E* **64** (2001) 016603, https://link.aps.org/doi/10.1103/PhysRevE.64.016603

44. H. F. Trotter, On the Product of Semi-Groups of Operators, *Proceedings of the American Mathematical Society* **10** (1959) 545, https://doi.org/10.2307/2033649

45. J. von Neumann and E. Wigner, Über merkwürdige diskrete Eigenwerte, *Phys. Z.* **30** (1929) 465 https://doi.org/10.1007/978-3-662-02781-3_19

46. N. Wiebe *et al*., Higher order decompositions of ordered operator exponentials, *Journal of Physics A: Mathematical and Theoretical* **43** (2010) 065203, https://dx.doi.org/10.1088/1751-8113/43/6/065203

47. W. Magnus and S. Winkler, Hill's Equation, Dover edition (Dover Publications Inc., Mineola, New York, 2004), pp. 49-80, https://books.google.com.mx/books?id=ML5wm-T4RVQC

48. K. Vogtmann, A. Weinstein, and V. Arnol'd, Mathematical Methods of Classical Mechanics, Graduate Texts in Mathematics (Springer, New York, 1997), pp. 1-580, https://books.google.com.mx/books?id=Pd8-s6rOt_cC

49. H. Broer and C. Simó, Resonance Tongues in Hill's Equations: A Geometric Approach, *Journal of Differential Equations* **166** (2000) 290, https://doi.org/10.1006/jdeq.2000.3804

50. M. Berry, Quantum chaology, not quantum chaos, *Physica Scripta* **40** (1989) 335, https://dx.doi.org/10.1088/0031-8949/40/3/013

51. Z. X. Liang, Z. D. Zhang, and W. M. Liu, Dynamics of a Bright Soliton in Bose-Einstein Condensates with Time-Dependent Atomic Scattering Length in an Expulsive Parabolic Potential, *Phys. Rev. Lett.* **94** (2005) 050402, https://link.aps.org/doi/10.1103/PhysRevLett.94.050402

52. N. Fabbri *et al*., Excitations of Bose-Einstein condensates in a one-dimensional periodic potential, *Phys. Rev. A* **79** (2009) 043623, https://link.aps.org/doi/10.1103/PhysRevA.79.043623

53. J. Stenger *et al*., Bragg Spectroscopy of a Bose-Einstein Condensate, *Phys. Rev. Lett.* **82** (1999) 4569, https://doi.org/10.1103/PhysRevLett.82.4569

54. A. D. Jackson, G. M. Kavoulakis, and E. Lundh, Stability of the solutions of the Gross-Pitaevskii equation, *Phys. Rev. A* **72** (2005) 053617, https://link.aps.org/doi/10.1103/PhysRevLett.82.4569

55. G. Roati *et al*., Anderson localization of a non-interacting Bose–Einstein condensate, *Nature* **453** (2008) 895, https://www.nature.com/articles/nature07071

56. J. Dujardin, T. Engl, and P. Schlagheck, Breakdown of Anderson localization in the transport of Bose-Einstein condensates through one-dimensional disordered potentials, *Phys. Rev. A* **93** (2016) 013612, https://link.aps.org/doi/10.1103/PhysRevA.93.013612